Dislocation Structure and Crystallite Size Distribution in Plastically Deformed Metals Determined by Diffraction Peak Profile Analysis

T. Ungár
G. Ribárik
J. Gubicza
P. Hanák

Department of General Physics,
Eötvös University Budapest,
H-1518, P.O.B. 32,
Budapest, Hungary

The dislocation densities and arrangement parameters and the crystallite size and size-distributions are determined in tensile or cyclically deformed polycrystalline copper specimens by X-ray diffraction peak profile analysis. The Fourier coefficients of profiles measured by a special high resolution X-ray diffractometer with negligible instrumental broadening have been fitted by the Fourier transforms of ab-initio size and strain profiles. It is found that in the fatigued samples the dislocations are mainly of edge type with strong dipole character. In the fatigued specimens the dislocation densities are found to be larger than in the tensile deformed samples when the saturation and flow stress levels are the same. [DOI: 10.1115/1.1418364]

1 Introduction

Dislocation structures are directly observed in micrographs obtained by transmission electron microscopy (TEM). These observations provide details on the micron scale. Comprehensive studies of the dislocation structures in plastically deformed metals have been carried out by different groups [1–3]. The average properties of the dislocation structures on the hundreds of microns up to millimeters scale, especially, some properties like long range internal stresses [4–7], dislocation densities [8–10], arrangement parameters [11,12] or statistical fluctuations [13–15] are better obtained by diffraction peak profile analysis [16].

Diffraction peaks broaden when crystallites are small or the material contains lattice defects. The diffraction order dependence of two effects is different enabling their separation. The two classical methods for this are: (i) the Williamson-Hall [17] and (ii) the Warren-Averbach [18] procedures. The first is based on the Full Widths at Half Maximum (FWHM) and the integral breadths while the second on the Fourier coefficients of the profiles. Both methods provide, in principle, apparent size parameters of crystallites or coherently diffracting domains and values of the mean square strain. The evaluations become, however, complicated if either the crystallite shape [19] or strain [20] are anisotropic. The mean square strain is often attempted to be given as a single valued quantity [18,21]. Experiment has shown, however, that the mean square strain, $\langle \varepsilon_{L,g}^2 \rangle$, is never a constant, neither as a function of L nor g, where L and g are the Fourier length (see below) and the absolute value of the diffraction vector, respectively [5–10,18,22–27]. The g dependence is further complicated by *strain anisotropy* which means that neither the breadth nor the Fourier coefficients of the diffraction profiles are monotonous functions of the diffraction angle or g [20,24,25,28–31].

In order to separate strain and size correctly strain anisotropy has to be treated properly. Two different models have been developed so far to this aim: (i) the phenomenological model based on the elastic anisotropy of crystals [30] and (ii) the dislocation model [24] based on the mean square strain of dislocated crystals [9,11,12]. Latter takes into account that the effect of dislocations on strain broadening depends on the relative orientations of the line and Burgers vectors of dislocations and the diffraction vector, similarly as the contrast effect of dislocations in electron microscopy. Anisotropic contrast can be summarized in contrast factors, C, which can be calculated numerically on the basis of the crystallography of dislocations and the elastic constants of the crystal [9,11,12,22,24,31–33]. Using the average contrast factors the *modified* Williamson-Hall and the *modified* Warren-Averbach procedures have been suggested [24], enabling to determine (i) different averages of crystallite sizes, (ii) the density and (iii) the effective outer cut off radius of dislocations [24,34]. A method has recently been developed to determine (a) crystallite size distribution and the dislocation structure in terms of (b) density, (c) arrangement parameter, and (d) character of dislocations [34].

In the present work, diffraction peak profile analysis is outlined briefly and applied to characterize the differences and/or similarities in the crystallite size distribution and in the average dislocation structure in copper specimens deformed either in tension or in fatigue.

2 Evaluation of Broadened Diffraction Peak Profiles

2.1 The Modified Warren-Averbach (mWA) Equation. According to the kinematical theory of diffraction the physical profiles of Bragg reflections are the convolution of the size and strain profiles [35]:

$$I^F = I^S * I^D, \tag{1}$$

where the superscripts F, S, and D refer to *physical*, *size*, and *strain* (*distortion*), respectively. (*physical profile* here means either that the measured profiles have been corrected for instrumental effects or that the instrumental effects are negligible.) The discrete Fourier transform of Eq. (1) is the Warren-Averbach equation [18]:

$$A_L = A_L^S A_L^D = A_L^S \exp[-2\pi^2 L^2 g^2 \langle \varepsilon_{g,L}^2 \rangle], \tag{2}$$

where L is the Fourier variable: $L = \mathrm{n}a_3$, n are integers and a_3 is the unit of the Fourier length in the direction of the diffraction vector $\mathbf{g}$: $a_3 = \lambda/[2(\sin\theta_2 - \sin\theta_1)]$, the diffraction profile is mea-

Contributed by the Materials Division for publication in the JOURNAL OF ENGINEERING MATERIALS AND TECHNOLOGY. Manuscript received by the Materials Division February 20, 2001; revised manuscript received May 21, 2001. Guest Editors: Mohammed Cherkaoui and László S. Tóth.

sured in the angular range θ_1 to θ_2 and λ is the wavelength of the X-rays. When strain is caused by dislocations the mean square strain is [11,12]:

$$\langle \varepsilon_{g,L}^2 \rangle = -(b/2\pi)^2 \pi \rho C f(\eta), \tag{3}$$

where ρ is the dislocation density, C is the contrast factor of dislocations, $\eta = L/R_e$, R_e is the effective outer cut-off radius of dislocations and $f(\eta)$ is a function derived explicitly by Wilkens for dislocations, see Eqs. A.6 to A.8 in [12]. For small values of η the Wilkens function can be approximated by a logarithmic function [6,7,9,11,12]:

$$\langle \varepsilon_{g,L}^2 \rangle \cong \frac{\rho C b^2}{4\pi} \ln(R_e/L), \tag{4}$$

Inserting (4) into the Warren-Averbach equation we obtain the *modified* Warren-Averbach equation [24]:

$$\ln A(L) \cong \ln A^S(L) - \rho B L^2 \ln(R_e/L)(K^2\bar{C}) + O(K^4\bar{C}^2). \tag{5}$$

2.2 The Contrast Factors of Dislocations. In a texture free cubic polycrystal or if the Burgers vector population on the different slip systems is random the contrast factors of dislocations can be averaged over the permutations of the hkl indices [32]:

$$\bar{C} = \bar{C}_{h00}(1 - qH^2), \tag{6}$$

where $\bar{C}_{h00}$ are the average dislocation contrast factors for the $h00$ reflections, $H^2 = (h^2k^2 + h^2l^2 + k^2l^2)/(h^2 + k^2 + l^2)^2$ and q is a parameter depending on the elastic constants of the crystal and on the edge or screw character of the dislocations [33].

2.3 The Modified Williamson-Hall Plot. In the classical Williamson-Hall procedure [17] the full width at half maximum (FWHM) or the integral breadths of profiles are plotted versus $K = 2 \sin\theta/\lambda$, where θ is the diffraction angle and λ is the wavelength of X-rays. The intercepts and the slopes of the regressions through the measured data should provide apparent size parameters and values of the mean square strain, respectively [17]. Due to strain anisotropy, however, the data points do not follow smooth curves making reliable regressions impossible. It can be shown that the anisotropic contrast of dislocations enables the rationalisation of strain anisotropy in terms of the *modified* Williamson-Hall plot [24]:

$$\Delta K \cong \alpha/D + (\pi T b^2/2)\rho^{1/2} K^2 \bar{C} + O(K^4\bar{C}^2), \tag{7}$$

where ΔK is either the FWHM or the integral breadth of profiles, D is the so-called apparent size parameter, α is 0.9 or 1 for the FWHM or the integral breadth and T is a constant depending on the effective outer cut-off radius of dislocations [24].

2.4 The Size-Distribution of Crystallites. A diffraction experiment measures the coherent length, l, of crystallites parallel to the diffraction vector. Denoting the volume fraction of columns of the length between l and $l + dl$ by $g(l)dl$ the intensity distribution of a diffraction profile in the absence of strain, i.e., of a *size* profile is [34,35]:

$$I^S(s) = \int_0^\infty \frac{\sin^2(\pi l s)}{l(\pi s)^2} g(l) dl, \tag{8}$$

where $s = \Delta(2\theta)/\lambda$. Assuming spherical crystallites and denoting the size-distribution density function by $f(x)$ [36]:

$$g(l) = Nl^2 \int_M^\infty f(x) dx, \tag{9}$$

where N is a normalization factor. Assuming log-normal size distribution density:

$$f(x) = \frac{1}{\sqrt{2\pi}\sigma} \frac{1}{x} \exp\left\{ -\frac{[\ln(x/m)]^2}{2\sigma^2} \right\}, \tag{10}$$

the *size* profile $I^S(s)$ is [34,36]:

$$I^S(s) = \int_0^\infty l \cdot \frac{\sin^2(\pi l s)}{2(\pi s)^2} \cdot \mathrm{erfc}\left[\frac{\ln(l/m)}{\sqrt{2}\sigma} \right] dl, \tag{11}$$

where m and σ are the median and the variance of $f(x)$ and erfc is the complementary error function.

2.5 The Determination of the Microstructural Parameters.

2.5.1 The Size Distribution of Crystallites Determined by the Modified Williamson-Hall and Warren-Averbach Procedures From the FWHM, the integral breadths and the Fourier transform of the measured profiles yield three apparent size parameters by the evaluation of Eqs. (5) and (7): D, d and L_0. On the other hand, the FWHM, the integral breadth and the Fourier transform of the *size* profile in Eq. (11), $I^S(q)$, provide numerically calculated values for the three apparent size parameters: $D^{m,\sigma}$, $d^{m,\sigma}$ and $L_0^{m,\sigma}$, each of which depend on m and σ. The calculated and the measured apparent size parameters can be matched by the least squares method in order to obtain the m and σ parameter values corresponding to the experimentally determined apparent size values:

$$(D^{m,\sigma} - D)^2 + (d^{m,\sigma} - d)^2 + (L_0^{m,\sigma} - L_0)^2 = \text{minimum}, \tag{12}$$

in which the fitting is carried out for m and σ. For spherical crystallites with log-normal size distribution the area-, volume- and arithmetically-weighted mean crystallite sizes are [37]:

$$\langle x \rangle_{\text{area}} = m \exp(2.5\sigma^2), \tag{13a}$$

$$\langle x \rangle_{\text{vol}} = m \exp(3.5\sigma^2), \tag{13b}$$

$$\langle x \rangle_{\text{arithm}} = m \exp(0.5\sigma^2). \tag{13c}$$

This simple and pragmatic procedure is believed to be more reliable than the methods in which either only the Fourier transform of profiles are used [38] or in which only two parameters of the profiles, e.g., the integral breadths and the Fourier transform are used.

2.5.2 The Dislocation Parameters Determined by the Modified Williamson-Hall and Warren-Averbach Procedures. From the *modified* Warren-Averbach equation in (5) and the *modified* Williamson-Hall plot in Eq. (7) the q parameter of the dislocation contrast factors, as defined in Eq. (6), can be determined. If the elastic constants of the material are known the experimental values of the q parameter enables the determination of the character of dislocations. In cubic crystals, for example, in terms of the volume fraction of screw or edge dislocations. The uncertainty in the determination of the value of the q parameter can be considerable thus the conclusions about the dislocation character have to be treated critically with respect to the experimental errors. The density and the arrangement parameter of dislocations, ρ and M, where $M = R_e\sqrt{\rho}$, can be determined from Eq. (5). The coefficients of the second term in the equation provide $\rho B L^2 \ln(R_e/L)$ as a function of L. Plotting these values versus $\ln L$ for small L values enables the graphic determination of ρ and R_e [39].

2.5.3 The Crystallite-Size and the Dislocation Parameters Determined by the Method of Multiple Whole Profile (MWP) Fitting [34,40]. The Wilkens function in Eq. (3), $f(\eta)$, together with the Fourier coefficients of the *size* profile in Eq. (11) enable the fitting of either the Fourier coefficients of the physical profiles in the entire range of L or the whole physical profiles themselves. The details of the Wilkens function can be found in the equations A.6 to A.8 in [12] and are reproduced [34,40]. A theoretical procedure [34] and the corresponding software [40] have been developed to fit the Fourier transforms of the experimentally determined physical peak-profiles by the product of the Fourier transforms of the *size* profile in Eq. (11) and the strain profile given by A_L^D, $\langle \varepsilon_{L,g}^2 \rangle$ and $f(\eta)$ in Eqs. (2) and (3). The procedure

can alternatively be used to fit the intensity distributions of measured profiles themselves. The Fourier transform of the *size* profile has been calculated in explicit form for spherical or ellipsoidal crystallite shape assuming log-normal size distribution [34,40]. Strain anisotropy is accounted for by scaling the strain profiles by $K^2\bar{C}$. The only fitting parameters in this procedure are the following microstructural quantities: (i) m and (ii) σ for the log-normal crystallite size distribution function, (iii) ρ and (iv) M, for the density and the arrangement parameter of dislocations, and (v) q for the average dislocation contrast factors in cubic crystals, respectively.

3 Experimental

3.1 Samples. Two pairs of four-nine (99.99 percent purity) OFHC polycrystalline copper specimens were deformed either by tension or cyclically to the same flow stress or saturation stress values of about 80 and 160 MPa, respectively. The stress and strain values are listed in the Table 1. The cyclic experiments were carried up to 2000 cycles, saturation was reached after the first few tens of cycles. It is assumed that in the fatigued samples a well developed cell structure with relatively narrow dislocation cell walls are developed [41]. The gauge length and diameter of the specimens was 16 and 6 mm, respectively. For the X-ray measurements cylinders of 4 mm height from the uniformly deformed regions were prepared. The measurements were performed on carefully polished and chemically etched surfaces perpendicular to the stress axis.

3.2 X-Ray Diffraction Technique. The diffraction profiles were measured by a special double crystal diffractometer with negligible instrumental broadening. A long fine focus copper anode of a sealed X-ray tube (Phillips) was operated as a line focus at 40 kV and 25 mA. The symmetrical 220 reflection of a Ge plane monochromator was used producing a parallel beam of about 100 μm thick foot print on the specimen. The $K\alpha_2$ component of the Cu radiation was eliminated by an 16 μm slit between the source and the Ge crystal. The profiles were registered by a linear position sensitive gas flow detector, OED 50 Braun, Munich. In order to avoid air scattering and absorption the distance between the specimen and the detector was overbridged by an evacuated tube closed by mylar windows. The distance between the specimen and the detector was set either at 500 or 300 mm depending on the width of the measured profiles.

4 Results and Discussion

In the present work, the measured profiles are evaluated by the Multiple Whole Profile (MWP) fitting procedure described in section 2.5.3. The measured and fitted Fourier coefficients and intensity distributions for the specimen tensile deformed to the flow stress and strain σ_{mech}=82 MPa and ε=0.045, respectively (Tensile 1, in Table 1) are shown in Fig. 1. The differences between the measured and fitted values are also shown in the lower parts of the figure. In Fig. 1(b) it can be seen that, though the differences between the measured a fitted intensities (in the lower part of the figure) are satisfactorily small, they have somewhat larger values for the 311 and 400 reflections. This has the following reason. Already at this strain level, ε=0.045, the dislocations are distributed heterogeneously. According to the composite model, in such dislocation structures long range internal stresses develop which are strongest in the ⟨100⟩ directions [4,41]. These long range internal stresses are manifested by pronounced asymmetries of the 200 and 311 diffraction profiles, especially in copper [5]. Here we note that the same effect is somewhat stronger in the specimen deformed to ε=0.166. The fitting procedure is carried out using the absolute values of the Fourier coefficients of the measured profiles and the fitted Fourier coefficients are all real. Obviously,

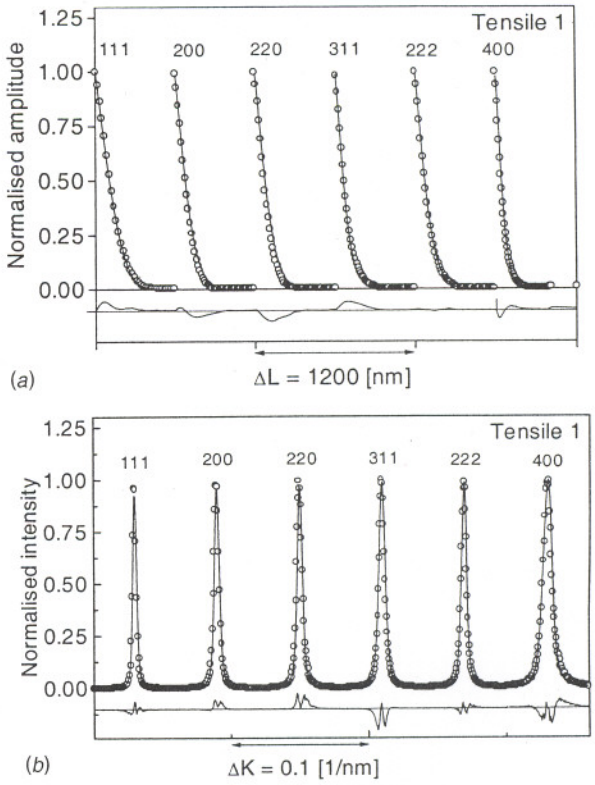

Fig. 1 (a) The measured (open circles) and the fitted theoretical (solid line) Fourier coefficients as a function of the Fourier variable *L* for the specimen deformed by tension to 82 MPa. The differences between the measured and fitted values are also shown in the lower part of the figure. The indices of the reflections are also indicated. (b) The measured intensity profiles (open circles) and the inverse Fourier transform of the fitted Fourier coefficients (solid lines) for the specimen deformed by tension to 82 MPa. The differences between the measured and fitted intensity values are also shown in the lower parts of the linear scale plots.

Table 1 The density, ρ, and the arrangement parameter, M, of dislocations, the q parameter of dislocation contrast factors, the median, m, and the variance, σ, of the crystallite size distribution and the volume weighted mean crystallite size for tensiled and fatigued specimens deformed to different levels of flow stress and saturation stress values, σ_{mech}. The values of the strain, ε, and the plastic strain amplitude, $\Delta\varepsilon_{pl}$, for tensile and cyclic deformation are also given.

Specimen	σ_{mech} [MPa]	ε; $\Delta\varepsilon_{pl}$	ρ [10^{14} m^{-2}]	M	q	m [nm]	σ	$\langle x\rangle_{vol}$ [nm]
Tensile1	82	0.045	0.3	2.1	1.8 ±0.1	316	0.21	370
Tensile2	164	0.166	3.6	1.5	1.93±0.1	129	0.20	150
Fatigue1	82	2.5×10^{-3}	3.9	0.32	1.67±0.1	123	0.36	200
Fatigue2	164	5×10^{-3}	5.8	0.33	1.67±0.1	129	0.38	215

the inverse Fourier transform of the fitted Fourier coefficients will be a symmetric profile deviating most from the measured profiles when the asymmetry is strongest, i.e., in the case of the 311 and 400 reflections.

The values of ρ, M, q, m, and σ obtained directly from the fitting procedure are listed in the Table 1. The volume average crystallite size, $\langle x \rangle_{vol}$, as defined in Eq. (13*b*) is also given in the table. The following conclusions can be drawn from the data. (i) The dislocation densities in the fatigued specimens are larger than in the tensile deformed ones when the flow stress is equal to the saturation stress. (ii) The dislocation arrangement parameter values, M, are considerably larger in the tensile deformed than in the fatigued states. (iii) The q parameter values are about 1.9 and 1.67 in the tensile deformed and in the fatigued states, respectively. (iv) The volume averaged crystallite size values decrease during deformation.

Taking into account that in the fatigued state the dislocation cell structure is well developed in which the thin cell walls have a volume fraction of about 0.1 [4] the local dislocation density in the cell walls of these samples is about $4-5\ 10^{15}\,m^{-2}$. In the tensile deformed specimens the cell walls are woolly, irregular and thick and have a volume fraction of about 0.25 to 0.4 [42]. This means that in these samples the local dislocation density in the cell walls is about $0.1-1\ 10^{15}\,m^{-2}$. The local dislocation density in the cell walls of the fatigued samples is by about a factor of 5 to 50 larger than in the tensile deformed specimens. This is in good correlation with both, the M and q parameter values. The value of M gives the strength of the dipole character of dislocations [11,12]: if M is small or large the dipole character and the screening of the displacements field of dislocations is strong or weak, respectively. At the same time, strong or weak screening and small or large values of M means strong or weak correlations in the dislocation distributions. The large and small values of M for the tensile deformed and fatigued samples means that in the fatigued samples the dipole character of dislocations is considerably stronger and the screening of displacement fields is much more effective than in the tensile deformed specimens. The possible q values were calculated numerically in [33] for Burgers vectors: $\mathbf{b}=a/2\langle 110\rangle$ for fcc crystals as a function of the elastic anisotropy, $A_z=2c_{44}/(c_{11}-c_{12})$, where c_{ij} are the elastic constants of the crystal. The q parameter values are distinctly different for edge or screw dislocations at a particular value of the Zener constant, A_z, as it can be seen from the figures in [33]. For copper $A_z=3.21$ and the q parameter values are 1.68 and 2.37 for pure edge and pure screw dislocations, respectively. The $q\cong 1.9$ value for the tensile deformed samples means that the dislocations are of mixed character. The $q\cong 1.6-1.7$ values for the fatigued samples mean that the dislocations are mainly of edge character. Both, (a) the stronger dipole and mainly edge character of dislocations in the fatigued samples and (b) the weak dipole and mixed character of dislocations in the tensile deformed samples are in good correlation with other observations, especially TEM experiments [1–4,42].

On the basis of the m and σ values in Table 1 and Eq. (10) the crystallite size distribution functions, $f(x)$, are drawn in Fig. 2. It can be seen that after a few percent tensile deformation (Tensile 1 specimen) the size distribution is at large x values and is broad. After about 17 percent deformation $f(x)$ shifts to lower x values and becomes somewhat narrower. The two fatigued samples reveal similar size distributions. The volume averaged crystallite size is about 400 nm in the sample tensile deformed to a few percent and this value decreases to about 200 nm in the samples deformed either in tension to 17 percent or in fatigue to $\Delta\varepsilon_{pl}=2.5-5\times 10^{-3}$. The average size of dislocation cells varies from one to a few microns in copper specimens deformed in these deformation regimes [1–4]. This apparent discrepancy between the average crystallite size obtained from peak broadening or observed in TEM micrographs has the following reasons. In a bulk specimens, like the copper samples investigated here, there is a

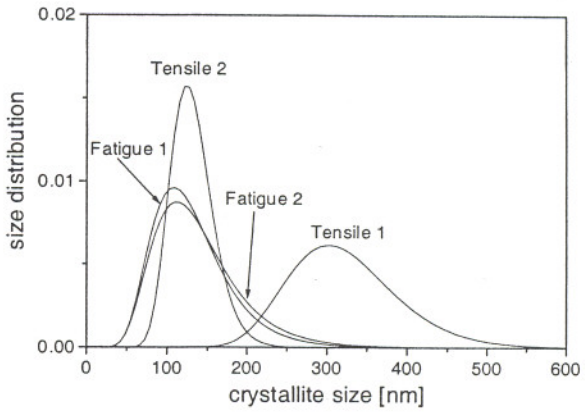

Fig. 2 Size distribution density-functions for the tensile deformed and the fatigued specimens

hierarchy of length scales [1,3]. In decreasing order they are: (i) grains, (ii) cell blocks, (iii) subgrains, (iv) dislocation cells, (v) cell interiors, (vi) cell boundaries, and (vii) distances between dislocations. (Note that, this hierarchy becomes more complicated for bulk materials with different phases, e.g., in alloys containing precipitates or in composites.) The misorientation between the different units of the microstructure can vary from zero through small angles to large angles. Crystallite size in X-ray diffraction is equivalent with the domains which are separated from the surrounding by a small misorientation, typically one or two degrees. The largest units in the microstructure are the grains where the adjacent units are separated by large angles. All other units from cell blocks down to cell boundaries can have very different misorientations ranging from a few tenths of degrees to any large value. The scales of misorientations within grains depends basically on the dislocation structure and arrangement inside the grains. Dipoles cause no misorientations, however, a few dislocations aligned in the configuration of small angle grain boundaries can produce misorientations of a few degrees. Due to this type of misorientation the scattering coherency of X-rays or neutrons can break down producing crystallite size values smaller than the grain size or even subgrain size observed in a TEM micrograph. A comparison of the average dislocation distances and the crystallite size obtained from the scattering experiment can tell to what extent the dislocations are arranged in dipoles or in arrangements producing misorientations.

Conclusions

A recently developed method of diffraction peak profile analysis has been applied to investigate the differences of the dislocation structure in tensile deformed and fatigued copper specimens and the following conclusions can be made.

1 The dislocation densities in the fatigued specimens are found to be larger than in the tensile deformed ones when the flow stress is equal to the saturation stress in good correlation with TEM observations in the literature.

2 The dislocation arrangement parameter values, M, are considerably larger in the tensile deformed than in the fatigued states indicating that in the fatigued samples the dislocations are arranged with more dipole character.

3 Strain anisotropy of peak broadening provided q parameter values of the dislocation contrast factors which are about 1.9 and 1.67 in the tensile deformed and in the fatigued states, corresponding to mixed and mainly edge dislocation character in the two different deformation modes, respectively.

4 Crystallite size and size-distributions have been determined and discussed in terms of dislocation caused misorientations and TEM observations.

Acknowledgments

The authors are grateful to Dr. Gy. Vörös and Mr. S. Kiss for their kind assistance in carrying out the mechanical testings. Thanks are due for the financial support of the Hungarian Scientific Research Fund, OTKA, Grant Nos. T031786, T029701 and D29339.

References

[1] Gil Sevillano, J., and Aernoudt, E., 1987, "Low Energy Dislocation Structures in Highly Deformed Materials," Mater. Sci. Eng., **86**, pp. 35–51.

[2] Bay, B., Hansen, N., Hughes, D. A., and Kuhlmann-Wilsdorf, D., 1992, "Evolution of fcc Deformation Structures in Polyslip," Acta Metall. Mater., **40**, pp. 205–219.

[3] Hughes, D. A., and Nix, W. D., 1989, "Strain Hardening and Substructural Evolution in Ni-Co Solid Solutions at Large Strains," Mater. Sci. Eng., **A122**, pp. 153–172.

[4] Mughrabi, H., 1983, "Dislocation Wall and Cell Structures and Long Range Internal Stresses in Deformed Metal Crystals," Acta Metall., **31**, pp. 1367–1379.

[5] Ungár, T., Mughrabi, H., Rönnpagel, D., and Wilkens, M., 1984, "X-Ray Line Broadening Study of the Dislocation Cell Structure in Deformed [001]-Oriented Copper Single Crystals," Acta Metall., **32**, pp. 333–342.

[6] Gaál, I., 1984, "Effect of Dislocation Distribution on the X-Ray Scattering from Deformed Metals," Proc. 5th Riso Int. Symp. on Metallurgy and Material Science, N. Hessel Andersen, M. Eldrup, N. Hansen, D. Juul Jensen, T. Leffers, H. Lilholt, O. B. Pedersen and B. N. Singh, eds., Riso National Lab., Roskilde, Denmark, pp. 249–254.

[7] Groma, I., Ungár, T., and Wilkens, M., 1988, "Asymmetric X-Ray Line Broadening of Plastically Deformed Crystals. Part I: Theory," J. Appl. Crystallogr., **21**, pp. 47–53.

[8] Krivoglaz, M. A., Martynenko, O. V., and Ryaboshapka, K. P., 1983, "Influence of correlation in position of dislocations on X-ray diffraction by deformed crystals," Phys. Met. Metallogr., **55**, pp. 1–12.

[9] M. A. Krivoglaz, 1996, *Theory of X-ray and Thermal Neutron Scattering by Real Crystals*, Plenum Press, N.Y. 1969; and *X-ray and Neutron Diffraction in Nonideal Crystals*, Springer-Verlag, Berlin Heidelberg, New York.

[10] Wilkens, M., and Bargouth, M. O., 1968, "Die Bestimmung der Versetzungsdichte verformter kupfer Einkristalle aus Verbreiterten Roentgenbeugungsprofilen," Acta Metall., **16**, pp. 465–468.

[11] Wilkens, M., 1970, "The Determination of Density and Distribution of Dislocations in Deformed Single Crystals from Broadened X-Ray Diffraction Profiles," Phys. Status Solidi A, **2**, pp. 359–370.

[12] M. Wilkens, 1970, "Theoretical Aspects of Kinematical X-ray Diffraction Profiles from Crystals Containing Dislocation Distributions," Fundamental Aspects of Dislocation Theory, J. A. Simmons, R. de Wit, R. Bullough, eds., Vol. II. Nat. Bur. Stand. (US) Spec. Publ. No. 317, Washington, DC, USA, pp. 1195–1221.

[13] Székely, F., Groma, I., and Lendvai, J., 2001, "Statistic Properties of Dislocation Structures Investigated by X-ray Diffraction," Mater. Sci. Eng., A, **309**, pp. 352–355.

[14] Groma, I., 1998, "X-ray Line Broadening Due to an Inhomogeneous Dislocation Distribution," Phys. Rev. B, **57**, pp. 7535–7542.

[15] Székely, F., Groma, I., and Lendvai, J., 2000, "Characterization of Self-Similar Dislocation Patterns by X-ray Diffraction," Phys. Rev. B, **62**, pp. 3093–3098.

[16] Wilkens, M., 1988, "X-ray diffraction line broadening and crystal plasticity," Proc. 8th Int. Conf. Strength Met. Alloys (ICSMA 8), Tampere, Finland, P. O. Kettunen, T. K. Lepistö, M. E. Lehtonen, eds., Pergamon Press, pp. 47–152.

[17] Williamson, G. K., and Hall, W. H., 1953, "X-Ray Line Broadening from Filed Aluminum and Wolfram," Acta Metall., **1**, pp. 22–31.

[18] Warren, B. E., and Averbach, B. L., 1950, "The Effect of Cold Work Distortions on X-ray Pattern," J. Appl. Phys., **21**, pp. 595–610.

[19] Louër, D., Auffredic, J. P., Langford, J. I., Ciosmak, D., and Niepce, J. C., 1983, "A Precise Determination of the Shape, Size and Distribution of Size of Crystallites in Zinc Oxide by X-ray Line Broadening Analysis," J. Appl. Crystallogr., **16**, pp. 183–191.

[20] Caglioti, G., Paoletti, A., and Ricci, F. P., 1958, "Choice of Collimators for a Crystal Spectrometer for Neutron Diffraction," Nucl. Instrum., **3**, pp. 223–228.

[21] Schwartz, L. H., and Cohen, J. B., 1977, *Diffraction from Materials*, Springer-Verlag, Berlin.

[22] Klimanek, P., and Kuzel, Jr., R., 1988, "X-Ray Diffraction Line Broadening due to Dislocations in Non-Cubic Materials. I. General Considerations and the Case of Elastic Isotropy Applied to Hexagonal Crystals," J. Appl. Crystallogr., **21**, pp. 59–66.

[23] van Berkum, J. G. M., Vermuelen, A. C., Delhez, R., de Keijser, T. H., and Mittemeijer, E. J., 1994, "Applicabilities of the Warren-Averbach Analysis and an Alternative Analysis for Separation of Size and Strain Broadening," J. Appl. Crystallogr., **27**, pp. 345–357.

[24] Ungár, T., and Borbély, A., 1996, "The effect of dislocation contrast on X-ray line broadening: a new approach to line profile analysis," Appl. Phys. Lett., **69**, pp. 3173–3175.

[25] Scardi, P., and Leoni, M., 1999, "Fourier modelling of the anisotropic line broadening of X-ray diffraction profiles due to line and plane lattice defects," J. Appl. Crystallogr., **32**, pp. 671–682.

[26] Chatterjee, P., and Sen Gupta, S. P., 1999, "Microstructural investigation of plastically deformed $Pb_{(1-x)}Sn_x$ alloys: an X-ray profile-fitting approach," J. Appl. Crystallogr., **32**, pp. 1060–1068.

[27] Cheary, R. W., Dooryhee, E., Lynch, P., Armstrong, N., and Dligatch, S., 2000, "X-ray diffraction line broadening from thermally deposited gold films," J. Appl. Crystallogr., **33**, pp. 1271–1283.

[28] Le Bail, A., and Jouanneaux, A., 1997, "A Qualitative Account for Anisotropic Broadening in Whole-Powder-Diffraction-Pattern Fitting by Second-Rank Tensors," J. Appl. Crystallogr., **30**, pp. 265–271.

[29] Dinnebier, R. E., Von Dreele, R., Stephens, P. W., Jelonek, S., and Sieler, J., 1999, "Structure of sodium para-hydroxybenzoate, $NaO_2C-C_6H_4OH$ by powder diffraction: application of a phenomenological model of anisotropic peak width," J. Appl. Crystallogr., **32**, pp. 761–769.

[30] Stephens, P. W., 1999, "Phenomenological Model of Anisotropic Peak Broadening in Powder Diffraction," J. Appl. Crystallogr., **32**, pp. 281–288.

[31] Wilkens, M., 1987, "X-ray Line Broadening and MeanSquare Strains of Straight Dislocations in Elastically Anisotropic Crystals of Cubic Symmetry," Phys. Status Solidi A, **104**, pp. K1–K6.

[32] Ungár, T., and Tichy, G., 1999, "The Effect of Dislocation Contrast on X-ray Line Profiles in Untextured Polycrystals," Phys. Status Solidi A, **171**, pp. 425–434.

[33] Ungár, T., Dragomir, I., Révész, A., and Borbély, A., 1999, "The Contrast Factors of Dislocations in Cubic Crystals: the Dislocation Model of Strain Anisotropy in Practice," J. Appl. Crystallogr., **32**, pp. 992–1002.

[34] Ungár, T., Gubicza, J., Ribárik, G., and Borbély, A., 2001, "Crystallite Size-Distribution and Dislocation Structure Determined by Diffraction Profile Analysis: Principles and Practical Application to Cubic and Hexagonal Crystals," J. Appl. Crystallogr., **34**, pp. 298–310.

[35] Guinier, A., 1963, *X-ray Diffraction*, Freeman, San Francisco, CA.

[36] Gubicza, J., Szépvölgyi, J., Mohai, I., Zsoldos, L., and Ungár, T., 2000, "Particle size distribution and the dislocation density determined by high resolution X-ray diffraction in nanocrystalline silicon nitride powders," Mater. Sci. Eng., A, **280**, pp. 263–269.

[37] Hinds, W. C. 1982. *Aerosol Technology: Properties, Behavior and Measurement of Airbone Particles*, Wiley, New York.

[38] Krill, C. E., and Birringer, R., 1998, "Estimating Grain-Size Distribution in Nanocrystalline Materials from X-ray Diffraction Profile Analysis," Philos. Mag. A, **77**, pp. 621–640.

[39] Ungár, T., Ott, S., Sanders, P. G., Borbély, A., and Weertman, J. R., 1998, "Dislocations, grain size and planar faults in nanostructured copper determined by high resolution x-ray diffraction and a new procedure of peak profile analysis," Acta Mater., **46**, pp. 3693–3699.

[40] Ribárik, G., Ungár, T., and Gubicza, J., 2001, "MWP-fit: a Program for Multiple Whole Profile Fitting Using Theoretical Functions," J. Appl. Crystallogr., **34**, pp. 669–676.

[41] Groma, I., and Mohammed, G., 2001, "Analysis of asymmetric broadening of X-ray line profiles caused by randomly distributed polarized dislocation dipoles and dislocation walls," Acta Mater., submitted for publication.

[42] Goettler, E., 1973, "Versetzungstruktur und Verfestigung von 100-Kupfereinkristallen I. Versetzungsanordnung und Zellstruktur zugverformter Kristalle," Philos. Mag., **28**, pp. 1057–1076.